

## MIT Open Access Articles

*Helix Bundle Loops Determine Whether Histidine Kinases Autophosphorylate in cis or in trans*

The MIT Faculty has made this article openly available. *Please share* how this access benefits you. Your story matters.

**Citation:** Ashenberg, Orr, Amy E. Keating, and Michael T. Laub. "Helix Bundle Loops Determine Whether Histidine Kinases Autophosphorylate in Cis or in Trans." *Journal of Molecular Biology* 425, no. 7 (April 2013): 1198–1209.

**As Published:** <http://dx.doi.org/10.1016/j.jmb.2013.01.011>

**Publisher:** Elsevier

**Persistent URL:** <http://hdl.handle.net/1721.1/101269>

**Version:** Author's final manuscript: final author's manuscript post peer review, without publisher's formatting or copy editing

**Terms of use:** Creative Commons Attribution-Noncommercial-NoDerivatives





Published as: *J Mol Biol.* 2013 April 12; 425(7): 1198–1209.

## Helix bundle loops determine whether histidine kinases autophosphorylate in *cis* or in *trans*

Orr Ashenberg<sup>1,2</sup>, Amy E. Keating<sup>1,2,4</sup>, and Michael T. Laub<sup>1,2,3,4</sup>

<sup>1</sup>Department of Biology, Massachusetts Institute of Technology, Cambridge, MA 02139

<sup>2</sup>Computational & Systems Biology Initiative, Massachusetts Institute of Technology, Cambridge, MA 02139

<sup>3</sup>Howard Hughes Medical Institute, Massachusetts Institute of Technology, Cambridge, MA 02139

### Abstract

Bacteria frequently use two-component signal transduction pathways to sense and respond to environmental and intracellular stimuli. Upon receipt of a stimulus, a homodimeric sensor histidine kinase autophosphorylates and then transfers its phosphoryl group to a cognate response regulator. The autophosphorylation of histidine kinases has been reported to occur both in *cis* and in *trans*, but the molecular determinants dictating which mechanism is employed are unknown. Based on structural considerations, one model posits that the handedness of a loop at the base of the helical dimerization domain plays a critical role. Here, we tested this model by replacing the loop from *E. coli* EnvZ, which autophosphorylates in *trans*, with the loop from three PhoR orthologs that autophosphorylate in *cis*. These chimeric kinases autophosphorylated in *cis*, indicating that this small loop is sufficient to determine autophosphorylation mechanism. Further, we report that the mechanism of autophosphorylation is conserved in orthologous sets of histidine kinases, despite highly dissimilar loop sequences. These findings suggest that histidine kinases are under selective pressure to maintain their mode of autophosphorylation, but can do so with a wide range of sequences.

### Introduction

Organisms must sense and respond to their environments to survive. In many cases, organisms use membrane-bound protein kinases to directly sense environmental stimuli and, in response, phosphorylate substrates that can effect cellular changes. These phosphorylation events are typically reversible, allowing for temporal control of protein function. In bacteria, the predominant phosphorylation-based systems are two-component signal transduction pathways, which involve a sensor histidine kinase and its cognate substrate, a response regulator.<sup>1</sup> Following activation by an input signal, a kinase homodimer autophosphorylates on a conserved histidine. The phosphoryl group is then transferred to a cognate response regulator, which can often trigger a transcriptional response inside cells. Many histidine kinases are bifunctional, and in addition to their kinase activity exhibit phosphatase activity toward their cognate regulators, allowing a system to reset once the input signal is removed.<sup>2</sup> Using these systems, prokaryotes can respond to a large and diverse array of

© 2013 Elsevier Ltd. All rights reserved.

<sup>4</sup>corresponding authors: laub@mit.edu, 617-324-0418; keating@mit.edu, 617-452-3398 .

**Publisher's Disclaimer:** This is a PDF file of an unedited manuscript that has been accepted for publication. As a service to our customers we are providing this early version of the manuscript. The manuscript will undergo copyediting, typesetting, and review of the resulting proof before it is published in its final citable form. Please note that during the production process errors may be discovered which could affect the content, and all legal disclaimers that apply to the journal pertain.

stimuli including light, carbon sources, quorum signals, antibiotics, and others.<sup>3</sup> Most bacteria encode dozens of paralogous histidine kinases and response regulators, with some encoding hundreds.<sup>4</sup>

The typical histidine kinase is an integral membrane homodimer with an extracytoplasmic sensory domain linked to a cytoplasmic transmitter domain through a transmembrane helix. Sensory domains are often members of the PAS or GAF family, but they show low sequence similarity owing to the diversity of inputs they recognize.<sup>5</sup> In contrast, the transmitter region of the kinase is highly conserved and always consists of a DHp (dimerization and histidine phosphotransfer) domain linked to a CA (catalytic and ATP binding) domain (Fig. 1A). The DHp domain includes two  $\alpha$ -helices that mediate homodimerization through the formation of a four-helix bundle.<sup>6</sup> The CA domain forms an  $\alpha/\beta$ -sandwich that binds ATP and catalyzes autophosphorylation of an exposed histidine residue in the DHp domain.<sup>7</sup>

Early studies of the model histidine kinase EnvZ from *E. coli* demonstrated that it autophosphorylates in *trans*, as the CA domain from one subunit of a homodimer phosphorylates the DHp domain of the other subunit (Fig. 1B).<sup>8</sup> *E. coli* kinases NtrB, AtoS, and CheA, *S. aureus* AgrC, and *A. tumefaciens* VirA also autophosphorylate in *trans*<sup>9-13</sup>, and all histidine kinases were initially assumed to function similarly. However, the kinases *T. maritima* HK853, *S. aureus* PhoR, and *E. coli* ArcB were recently shown to autophosphorylate exclusively in *cis* (Fig. 1B), *i.e.* the CA domain from one subunit autophosphorylates the DHp domain of the same subunit (although these kinases still homodimerize).<sup>14,15</sup> Whether these two mechanisms of autophosphorylation have functional consequences for signaling, and what determines whether a kinase autophosphorylates in *cis* or in *trans*, are currently unknown.

One model, suggested by histidine kinase structures, is that autophosphorylation mechanism is determined by the loop at the base of the DHp domain four-helix bundle.<sup>15</sup> This loop connects two  $\alpha$ -helices ( $\alpha 1$  and  $\alpha 2$ ) and changes in this loop's connectivity will change the handedness of the four-helix bundle. Here, handedness is defined by whether  $\alpha 2$  is positioned to the right or left of  $\alpha 1$  when looking down the axis of the four-helix bundle from its N-terminus (Fig. 1B).<sup>16</sup> Because the DHp loop determines the positioning of  $\alpha 2$  relative to  $\alpha 1$ , in this work we refer to a loop as right-handed when it is found in a right-handed four-helix bundle, with a similar definition applied to left-handed loops. The DHp loop is right-handed in *E. coli* EnvZ, which autophosphorylates in *trans*, but left-handed in *T. maritima* HK853, which autophosphorylates in *cis* (Fig. 1A-B); for each kinase, independent structural studies have consistently agreed on their respective loop handedness.<sup>6,15,17,18</sup> Differences in loop handedness are not expected to significantly change the structure of the helix bundle itself, but can readily change whether the ATP bound by a CA domain of one subunit is closer to the autophosphorylation site of the same subunit or the opposite subunit (Fig. 1B).<sup>19</sup> Although the CA domain can move relative to the DHp domain, the flexible linker between these domains is too short to readily allow phosphorylation of both histidines in a DHp dimer by a single CA domain.

The sequence of the DHp domain loop is highly variable, even when comparing orthologous histidine kinases (Fig. 2A). Such diverse sequences might be expected to give rise to variability in the handedness of their structures, and consequently variability in whether the kinase autophosphorylates in *cis* or in *trans*. Here, we tested whether autophosphorylation mechanism is conserved among orthologs of the *E. coli* kinases EnvZ and PhoR.<sup>8,15</sup> Surprisingly, we found that the mode of autophosphorylation is highly conserved, and that orthologs of EnvZ and PhoR with diverse loops autophosphorylated in *trans* and in *cis*, respectively. We also found that the loops from kinases that autophosphorylate in *cis* are sufficient, when transplanted into EnvZ, to change autophosphorylation mechanism from in

*trans* to in *cis*. Together, our findings indicate that the DHp loop is a functionally important determinant of autophosphorylation mechanism in histidine kinases, supplanting the notion that these loops are simple linkers between helices.

## Results

### Methodology for determining whether autophosphorylation occurs in *cis* or in *trans*

To determine whether a kinase autophosphorylates in *cis* or in *trans*, we characterized the *in vitro* autophosphorylation of heterodimers comprising one wild-type subunit (WT) and one mutant subunit (MUT) that cannot bind ATP because it harbors an alanine in place of a conserved glycine in the G2 box of the CA domain (Fig. 1C).<sup>9,20</sup> If a kinase autophosphorylates exclusively in *cis*, then only the wild-type subunit in the heterodimer will be phosphorylated. If a kinase autophosphorylates in *trans*, then only the mutant subunit in the heterodimer will be phosphorylated (Fig. 1C). Thus, distinguishing between autophosphorylation in *trans* and in *cis* can be determined by assessing whether the mutant or wild-type subunit, respectively, is autophosphorylated. To distinguish the subunits, we fused CFP to the N-terminus of the wild-type subunit and a smaller FLAG epitope to the N-terminus of the mutant subunit. Autophosphorylation was detected through addition of [ $\gamma$ -<sup>32</sup>P]ATP followed by resolution of WT and MUT subunits with SDS-PAGE. The observed autophosphorylation represents a baseline activity as no input stimuli were added.

To form the heterodimer, homodimeric wild-type and mutant kinases were mixed together. As such a mixture equilibrates, three different dimers can form: the two possible homodimers and a heterodimer. We added 10-fold excess of the mutant kinase to favor formation of mutant homodimer and the heterodimer. The mutant homodimer cannot bind ATP, so any autophosphorylation activity observed should stem primarily from the heterodimer. For kinases that operate in *trans*, the mutant kinase chain in the heterodimer will be phosphorylated. For kinases that operate in *cis*, the wild-type kinase chain in the heterodimer will be phosphorylated. However, modification of the wild-type chain could also result from in *trans* phosphorylation in a small population of wild-type dimer. Thus, to confirm cases of autophosphorylation in *cis*, we compared time courses for the wild-type kinase alone or in the presence of excess mutant kinase (Fig. 1C). Under the assumption that the activity of the wild-type kinase is the same in a WT homodimer or a WT-MUT heterodimer, similar time courses strongly support an in *cis* mechanism.

Heterodimer formation in our assay results from subunit exchange following mixing of the wild-type and mutant kinases, and we measured the kinetics of this exchange using a previously developed FRET assay.<sup>21</sup> Briefly, we mixed CFP- and YFP-tagged versions of a wild-type kinase in the absence or presence of mutant kinase, and measured the change in FRET signal over time (for details, see Methods) (Supp. Fig. 1A). This assay confirmed that the wild-type and mutant kinases were competent to interact and indicated the appropriate equilibration time necessary to form heterodimers.

### Autophosphorylation mechanism is conserved among EnvZ and PhoR orthologs

*E. coli* EnvZ autophosphorylates in *trans* and *S. aureus* PhoR autophosphorylates in *cis*.<sup>8,15</sup> To assess whether the mechanisms are conserved, we examined autophosphorylation of four EnvZ orthologs and nine PhoR orthologs taken from phylogenetically diverse organisms (Supp. Table 1). An alignment of the DHp domains from these orthologs highlights the diversity of the loops relative to the conservation in the two  $\alpha$ -helices,  $\alpha$ 1 and  $\alpha$ 2 (Fig. 2A). Even for orthologs from the same proteobacterial subdivision, such as *E. coli* EnvZ and *P. aeruginosa* EnvZ ( $\gamma$ -proteobacteria) or *D. vulgaris* PhoR and *G. sulfurreducens* PhoR ( $\delta$ -proteobacteria), there is often significant diversity in the loop sequences.

For each EnvZ and PhoR ortholog, we purified a wild-type construct and an ATP-binding-deficient construct, each harboring the DHp and CA domains. The transmembrane and periplasmic domains were not included; however, those domains likely do not influence autophosphorylation mechanism.<sup>8,14,22</sup> We used the FRET assay described above to determine the time necessary to form sufficient heterodimer after mixing the two homodimers. For each kinase, the FRET signal formed by CFP- and YFP-tagged wild-type kinase was significantly reduced by addition of untagged mutant kinase (Supp. Fig. 1). Some kinases, like *P. aeruginosa* EnvZ, underwent subunit exchange within minutes whereas others, like *E. coli* PhoR, underwent subunit exchange over several hours (Supp. Fig. 1). This broad range of subunit exchange times for different kinases is consistent with previous reports.<sup>9,22,23</sup>

After allowing heterodimers to form using the equilibration times indicated by the FRET assay, we tested the autophosphorylation mechanism for each EnvZ ortholog. We observed autophosphorylation for each wild-type EnvZ ortholog but not any of the mutated variants when incubated alone, as expected (Fig. 3A). When the wild-type and mutant kinases were mixed together, the mutant subunit was strongly phosphorylated in each case, clearly indicating that phosphorylation in the heterodimer occurred in *trans*. This result indicates that the autophosphorylation mechanism for EnvZ is likely conserved, at least across  $\alpha$ - and  $\gamma$ -proteobacteria.

We then carried out the same experiments with PhoR orthologs. For each ortholog, when the wild-type and mutant constructs were mixed together to form heterodimers, only the wild-type subunit was significantly phosphorylated, suggesting that each PhoR ortholog autophosphorylated in *cis* (data not shown). To confirm these results and a *cis* autophosphorylation mechanism, we performed time-course experiments to compare the rate of autophosphorylation of the heterodimer with the wild-type homodimer. For five of the nine orthologs (*B. thailandensis*, *B. subtilis*, *B. fragilis*, *G. sulfurreducens*, *S. aureus*), the rates were similar, strongly supporting the conclusion that these kinases autophosphorylated in *cis* (Fig. 3B, Supp. Fig. 2). For three PhoR orthologs (*E. coli*, *C. crescentus*, *S. coelicolor*), the rate of heterodimer autophosphorylation was moderately reduced relative to the homodimer. This reduction in phosphorylation could indicate that the WT-MUT heterodimer is less active than the wild-type homodimer, or that mutant kinase present in these mixtures can inhibit phosphorylation of the heterodimer. To test the latter possibility, we mixed wild-type *E. coli* and *C. crescentus* PhoR with their corresponding MUT variants, but omitted the equilibration step such that very little heterodimer formed (Supp. Fig. 1). A similar decrease in autophosphorylation occurred (Supp. Fig. 3), indicating that the wild-type PhoR constructs were partially inhibited simply by the presence of mutant protein, perhaps through dimer-dimer interactions. Finally, for one PhoR construct (*D. vulgaris*), autophosphorylation of the heterodimer was moderately higher than that of the homodimer.

In sum, for all nine PhoR orthologs, our data indicate that autophosphorylation occurs in *cis*. In three cases (*B. subtilis*, *C. crescentus*, *D. vulgaris*), we observed a faint band corresponding to phosphorylation of the mutant chain (Fig. 3B). This band may indicate low rates of autophosphorylation in *trans*. Alternatively, it could result from dimer-dimer interactions and the phosphorylation of a mutant chain in one dimer by a wild-type chain from another dimer. Whatever the case, the mutant band was consistently much less intense than the wild-type band, supporting the conclusion that PhoR orthologs autophosphorylate primarily in *cis*.

### Autophosphorylation mechanism of loop chimeras

The DHp domains of *E. coli* EnvZ, which autophosphorylates in *trans*, and *T. maritima* TM853, which autophosphorylates in *cis*, both adopt four-helix bundle structures, but the

loop connecting  $\alpha$ -helices 1 and 2 in the two structures have different handedness.<sup>6,17</sup> To test whether differences in loops are related to the difference in autophosphorylation mechanism, we constructed chimeras in which we replaced the loop from *E. coli* EnvZ, with three diverse loops from *E. coli* PhoR, *B. fragilis* PhoR, or *S. aureus* PhoR, each of which autophosphorylates in *cis* (Fig. 2B). We also replaced the loop from *E. coli* EnvZ with that from *E. coli* RstB, another kinase that autophosphorylates in *trans* (Fig. 2B, 4A). Because there are no structures of the PhoR orthologs or of RstB, we do not know the exact boundary between helix and loop, so our chimeras may have introduced a small number of helical residues flanking the DHp loop.

The three EnvZ-PhoR chimeras each had autophosphorylation rates comparable to *E. coli* EnvZ, and reached their maximum level of autophosphorylation after ~5 minutes, indicating that the loop swaps did not significantly affect overall autokinase activity (Fig. 4B, Supp. Fig. 4). To test whether these chimeras autophosphorylated in *cis* or in *trans*, we mixed each chimera with its corresponding ATP-binding-deficient mutant, as above. In each case, we continued to see high rates of autophosphorylation, with a single band corresponding to the kinase-active chain (Fig. 4B), indicating that autophosphorylation occurred in *cis*. For the chimera containing the loop from *E. coli* PhoR, the WT-MUT mixture showed reduced phosphorylation at time points beyond 2 minutes (Fig. 4B, Supp. Fig. 4). However, an alternate chimera that included additional, loop-proximal residues from *E. coli* PhoR (*E. coli* EnvZ-*E. coli* PhoR\*) autophosphorylated in *cis* with little reduction in activity (Supp. Fig. 5).

Finally, we tested the EnvZ-RstB chimera and found that it autophosphorylated in *trans*, like the wild-type EnvZ and RstB kinases from which it was derived (Fig. 4A). Taken together, our results demonstrate that the loop in the DHp domain of a histidine kinase is sufficient to change kinase autophosphorylation mechanism from operating in *trans* to in *cis*.

### Loop swaps change dimerization specificity but not phosphotransfer specificity

We next assessed whether the EnvZ-RstB and EnvZ-PhoR loop chimeras showed any changes in kinase dimerization specificity as previous studies had demonstrated that histidine kinases specifically form homodimers *in vitro*.<sup>21</sup> We tested whether the chimeras could interact with *E. coli* EnvZ, using a FRET assay that allows fitting of equilibrium dissociation constants for both homodimers and heterodimers.<sup>21</sup> This assay was performed in a competitive-inhibition format, where the FRET signal from a mixture of CFP- and YFP-labeled *E. coli* EnvZ was inhibited by increasing concentrations of unlabeled, mutant kinase (Fig. 5A). We found that the chimera homodimers were similar in stability to the EnvZ homodimer, with dissociation constants ranging from ~0.1  $\mu$ M to 0.5  $\mu$ M (Fig. 5A, Supp. Fig. 6, Supp. Table 2). However, the heterodimers formed between EnvZ and the chimeras showed marked differences. The EnvZ-RstB chimera, which autophosphorylates in *trans* like EnvZ, interacted tightly with EnvZ. But the EnvZ-PhoR chimeras, which autophosphorylate in *cis*, interacted with EnvZ with dissociation constants approximately one order of magnitude weaker.

We also tested whether the EnvZ-RstB and EnvZ-PhoR loop chimeras still interacted with OmpR, the cognate response regulator for EnvZ. Previous work established that kinases specifically phosphotransfer to their cognate response regulators *in vitro*.<sup>24</sup> We measured the phosphotransfer activity of the chimeric kinases by incubating each kinase with *E. coli* OmpR and [ $\gamma$ -<sup>32</sup>P]ATP. Wild-type *E. coli* EnvZ phosphorylates its cognate response regulator OmpR *in vitro*, as manifested by a significant and rapid decrease in phosphorylated EnvZ upon addition of OmpR (Fig. 5B). Phosphorylated kinase incubated in the absence of response regulator showed no decrease in phosphorylation signal (Fig. 5B). Note that a strong band corresponding to OmpR is not expected, because EnvZ also drives



the dephosphorylation of OmpR~P after phosphotransfer. Each chimera demonstrated robust phosphotransfer to OmpR indicating that the change in loop and consequent change in autophosphorylation mechanism did not affect interaction between the kinase and its cognate response regulator.

## Discussion

By constructing and analyzing various histidine kinases and kinase chimeras, we found that the loop in the DHp domain is a key molecular determinant of autophosphorylation mechanism. Given this observation, it is striking that orthologous kinases with widely divergent loop sequences have conserved their autophosphorylation mechanism. Below we discuss the functional role of the loops and possible selective pressures influencing whether histidine kinases autophosphorylate in *cis* or in *trans*.

### Kinase loops as determinants of autophosphorylation mechanism

Introducing loops from PhoR orthologs that autophosphorylate in *cis* into an EnvZ ortholog that autophosphorylates in *trans* caused a switch in autophosphorylation mechanism. As an explanation for this observation, we favor a model in which the directionality of the loop connecting the helices is central to establishing autophosphorylation in *cis* or in *trans* (Fig. 1B). *E. coli* EnvZ has a right-handed loop and autophosphorylates in *trans*, and *T. maritima* HK853 has a left-handed loop and autophosphorylates in *cis*.<sup>6,15</sup> Based on a loop-handedness model, we expect the EnvZ orthologs, *E. coli* RstB, and the EnvZ-RstB chimera to have right-handed loops, and we expect the PhoR orthologs and the EnvZ-PhoR chimeras to have left-handed loops. Future structural studies will be needed to test these predictions.

The *B. subtilis* kinase DesK could be an exception to the loop-handedness model. DesK has a left-handed loop, similar to that seen in HK853, but was suggested to autophosphorylate in *trans* based on cross-linking studies.<sup>25</sup> However, cross-linking can potentially report on dimer-dimer interactions rather than interactions within a dimer. Phosphotransfer experiments similar to those performed here are needed to unambiguously determine the mechanism of DesK autophosphorylation. DesK could also function differently from other histidine kinases. Notably, the linker between the DHp and CA domains in DesK is 15 residues shorter than in HK853.<sup>19</sup> The length and structure of this linker may influence which DHp domain a given CA domain can autophosphorylate.

Loop handedness could be influenced by several sequence properties, including loop length and loop physicochemical characteristics. The DHp loop in *E. coli* EnvZ (*trans*) is shorter than that in *T. maritima* HK853 (*cis*), and interestingly, the loops from EnvZ orthologs we characterized are often predicted by PSIPRED to be shorter than the loops from PhoR orthologs (4-5 vs. 6-7 residues) (Supp. Fig. 7).<sup>26</sup> Local structural motifs in the loop region could also correlate with or specify loop handedness. In particular, short 3<sub>10</sub> helices follow the C-terminus of the first helix in *T. maritima* HK853 and precede the N-terminus of the second helix in *E. coli* EnvZ. A bend at the junction between the two helix types contributes to the turn structure in these kinases, and this may favor one loop handedness over another.<sup>17,18,27</sup> Characterizing the autophosphorylation mechanism for kinases with existing structures, like KinB or ThkA, could further support the loop-handedness model and provide additional information about how loop sequence encodes handedness.<sup>28,29</sup>

Although we favor a model in which loop sequence influences loop handedness which, in turn, dictates autophosphorylation mechanism, we cannot rule out other possibilities. For instance, changes in loop sequence could affect the dynamics of the DHp domain. This domain undergoes conformational changes upon receipt of an input signal, and hydrogen/deuterium exchange experiments performed with *E. coli* EnvZ identified changes in helicity

near the autophosphorylation site that accompany changes in osmolality.<sup>30</sup> It is possible that loop sequence and structure affect the structural dynamics of the DHP domain and, consequently, whether autophosphorylation occurs in *cis* or in *trans*. However, a variety of structural studies indicate that structural changes in DHP domains are largely restricted to the top half of the helix bundle, while the bottom half containing the loops remains relatively static.<sup>19</sup> This makes a model in which loop handedness dictates the positioning of the CA and DHP domains (Fig. 1B) seem more likely.

### Conservation of autophosphorylation mechanism

The EnvZ and PhoR orthologs we characterized come from bacterial species that, in some cases, diverged from one another hundreds of millions of years ago. However, we found that their autophosphorylation mechanisms are conserved, despite highly dissimilar loop sequences. This conservation across long periods of time suggests that the mechanism of histidine kinase autophosphorylation may be under selection. Why different kinases would be under pressure to retain different mechanisms is unclear, because in either in *cis* or in *trans* autophosphorylation the same product is made, a phosphorylated histidine available for phosphotransfer to a cognate response regulator. A possible explanation is that other kinase functions linked to DHP loop handedness, separate from autophosphorylation mechanism, are under selection.

One possibility is that loop handedness may contribute to specificity in histidine-kinase dimerization interactions, thereby promoting the isolation of signaling pathways.<sup>31</sup> For example, EnvZ and its paralog RstB were previously shown to specifically form homodimers. Presumably, a heterodimer between these two kinases would lead to detrimental cross-talk between their respective pathways.<sup>21</sup> An *E. coli* EnvZ-RstB loop chimera, identical to the one in this study, maintained an interaction with EnvZ. This suggested that loop swaps do not affect kinase dimerization. However, loop changes in the three EnvZ-PhoR chimeras characterized here did lead to differences in dimerization. Interactions of EnvZ with the EnvZ-PhoR chimeras were destabilized relative to the interaction of EnvZ with the EnvZ-RstB chimera (Fig. 5A). The loop model supported by this work suggests that RstB has a right-handed loop, like EnvZ, whereas PhoR and the EnvZ-PhoR chimeras have left-handed loops. It appears that mixed dimers between kinases with different loop handedness are destabilized. Possible reasons for this are illustrated in Fig. 5C, which shows that such kinases would be unable to form the stereotypical dimer. Either residues that are normally solvent exposed would become buried in the helix-bundle core, or the  $\alpha 1$  and  $\alpha 2$  helices would not be correctly positioned relative to one another in the helix bundle. Avoiding these highly atypical arrangements could require that the loop adopt a higher energy conformation. Destabilization of mixed dimers via this mechanism could also contribute to kinase pathway isolation. After gene duplication, a new histidine kinase could change its DHP loop handedness as one step towards evolving dimerization specificity against its new paralog. Conserving the changed loop handedness, and the resulting autophosphorylation mechanism, could be important for maintaining dimerization specificity.

Loop handedness may also play a role in phosphotransfer specificity. Loop changes in the chimeras were neutral with respect to phosphotransfer specificity, both here (Fig. 5B) and in earlier studies.<sup>32</sup> However, in earlier work that aimed to change the phosphotransfer specificity of kinases by making mutations at the base of their DHP helix bundles, it was observed that accompanying changes in the loops were sometimes required.<sup>32</sup> For example, rewiring EnvZ to phosphorylate PhoB, the cognate response regulator of PhoR, required introduction of the PhoR loop into EnvZ.<sup>32</sup> We suggest a model in which the binding mode of the response regulator can be somewhat different for kinases with different loop handedness. Based on the structure of *cis* kinase HK853 in complex with its cognate



response regulator, the EnvZ-PhoR chimeras likely contact the regulator using the  $\alpha 1$  and  $\alpha 2$  helices from the same chain in their DHP domain dimers (Fig. 5B).<sup>15</sup> Interestingly, a few positions in the DHP loop from HK853 (S279, E282, L283, and T287) also contact the regulator, adding to the kinase-regulator interface. In the EnvZ-PhoR chimera, similar specific contacts made by the PhoR loop may have been required in switching EnvZ phosphotransfer specificity to PhoB. In contrast, a *trans* kinase like EnvZ likely interacts with its response regulator using the  $\alpha 1$  helix of one chain and the  $\alpha 2$  helix of the partner chain in its DHP domain dimer (Fig. 5B). In this arrangement, the DHP loop is not close to the interface with the regulator and is perhaps less important for determining binding specificity. This model is supported by the observation that rewiring EnvZ to phosphorylate RstA, the cognate regulator of RstB, did not require changing the loop.<sup>32</sup> It is also consistent with our observation here, that EnvZ-PhoR chimeras could phosphorylate OmpR, because the interaction between *E. coli* EnvZ and OmpR is not expected to require a loop contact. These arguments suggest that loop handedness could help insulate pathways by destabilizing certain kinase-response regulator interactions that lack key loop interactions.

In closing, we emphasize that although our study supports a conservation of mechanism, the autophosphorylation mechanisms of most kinases are not known. Including our work here, 20 histidine kinases now have a characterized autophosphorylation mechanism. But there are tens of thousands of kinases. A predictive rule for autophosphorylation mechanism, which could possibly be established by studying determinants of loop handedness, would help establish this trend of conservation more broadly across kinase families.

## Methods

### Cloning and protein purification of kinase orthologs and chimeras

PhoR orthologs (341 sequences) and EnvZ orthologs (762 sequences) were previously identified by a reciprocal best BLAST hit procedure, using full-length sequences as the queries.<sup>33</sup> Ortholog sequences were aligned using ClustalW.<sup>34</sup> When calculating sequence conservation and information content for each position in the DHP domain, a sequence alignment of all available orthologs was filtered such that no pair of sequences was greater than 90% identical.<sup>35</sup> When predicting loop lengths, PSIPRED was run using a database of histidine kinase sequences downloaded from the Pfam database (family PF00512) and filtered for sequence redundancy.<sup>26,36</sup> Predictions were made for all EnvZ and PhoR orthologs characterized in this study, and for *E. coli* AtoS, *E. coli* RstB, *E. coli* NtrB, and *T. maritima* HK853, which are all members of the same major kinase subfamily as EnvZ and PhoR.<sup>37</sup>

For each identified kinase ortholog, pENTR clones for use in the Gateway recombination cloning system were generated as previously described from genomic DNA.<sup>21</sup> The amino acid boundaries for each kinase are listed in Supplementary Table 1. Each clone contained the kinase DHP and CA domains. Some EnvZ or PhoR orthologs have a cytoplasmic HAMP or PAS domain, respectively, N-terminal to their DHP domain. The HAMP domain was included in the *S. meliloti* EnvZ construct, and the PAS domain was included in the *E. coli*, *C. crescentus*, and *B. subtilis* PhoR constructs. To construct EnvZ-PhoR loop chimeras, the loop region of *E. coli* EnvZ was replaced by PhoR loop sequences using PCR-based site-directed mutagenesis as previously described.<sup>21</sup> Each ortholog or chimera was then cloned into His<sub>6</sub>-expression vectors encoding either N-terminal ECFP (pRG31) or N-terminal monomeric YFP (pRG88).<sup>21,38</sup> The pRG31 clones are referred to as wild-type (WT) constructs.

To disrupt ATP binding by the kinase, the third glycine in the G2 box (G×G×G) of the CA domain was mutated to alanine using QuikChange site-directed mutagenesis (Stratagene).

The mutant construct (MUT), used in the autophosphorylation and FRET-based assays, was created by taking this resulting construct and adding a tandem FLAG tag (DYKDDDDKDYKDDDDKGS) to the N-terminus using PCR. These pENTR clones were recombined into a His<sub>6</sub>-expression vector, pHis-DEST, using the Gateway LR clonase reaction.<sup>24</sup> Full-length response regulator *E. coli* OmpR was previously cloned into a His<sub>6</sub>-expression vector, pTRX-HIS-DEST.<sup>24</sup> Protein expression and protein purification were performed as previously described.<sup>21</sup>

### FRET equilibration assay

To determine appropriate equilibration times for the autophosphorylation assays, interaction between CFP-histidine kinase (WT) and FLAG<sub>2</sub>-mutant histidine kinase (MUT) was monitored by measuring changes in FRET (fluorescence resonance energy transfer) signal over time. FLAG<sub>2</sub>-mutant histidine kinase at 50 μM was added to an equimolar mixture of CFP-histidine kinase and YFP-histidine kinase at 5 μM in HEPES storage buffer (10 mM HEPES-KOH pH 8.0, 50 mM KCl, 10% glycerol, 0.1 mM EDTA, 1 mM DTT). These mixtures were prepared in 96-well plates (Corning), covered with a foil seal, and incubated at 30 °C. Fluorescence in each well was measured over time using a Varioskan plate reader at 30 °C. To measure FRET signal, three channels were monitored: donor channel (excite 433 nm, emit 475 nm), acceptor channel (excite 488 nm, emit 527 nm), and FRET channel (excite 433 nm, emit 527 nm). In each well at the indicated time, 5 fluorescence measurements were made in each channel and then averaged. A corrected FRET emission signal was calculated as previously described.<sup>21</sup> The equilibration times chosen for the autophosphorylation assay are listed in Supplementary Table 1 and marked in Supplementary Figure 1. Each FRET equilibration assay was performed at least twice, and results were similar across duplicates.

### Determining autophosphorylation mechanism

To demonstrate whether a kinase ortholog autophosphorylated in *trans*, 5 μM wild-type CFP-kinase (WT) was mixed in the absence or presence of 50 μM FLAG<sub>2</sub>-mutant kinase (MUT) in HEPES storage buffer plus 5 mM MgCl<sub>2</sub>. The mixtures were equilibrated at 30 °C according to times established by the FRET equilibration assay (Supplementary Table 1). As a negative control, 50 μM mutant kinase was also equilibrated. After equilibration, the mixtures were autophosphorylated with 500 μM ATP and 5 μCi [ $\gamma$ -<sup>32</sup>P]ATP (Amersham Biosciences, 6000 Ci/mmol) for 30 min at 30 °C. Autophosphorylation was stopped by adding 4X sample buffer (500 mM Tris pH 6.8, 8% SDS, 40% glycerol, 400 mM  $\beta$ -mercaptoethanol), and mixtures were placed on ice before being separated on a 10% Tris-HCl SDS-PAGE gel (Bio-Rad). The gel was exposed to a phosphor screen for 2 h at room temperature, the resulting screen was scanned using a Storm 860 imaging system (Amersham Biosciences) at 50 μm resolution, and the images were quantified with ImageQuant 5.2.

To demonstrate a kinase ortholog autophosphorylated in *cis*, the same procedure as in the previous paragraph was performed; the only difference was that the autophosphorylation reaction was tracked over time. At each time point, an aliquot of the autophosphorylation mixture was removed, and the reaction was stopped by adding sample buffer. The autophosphorylation time-courses of 5 μM wild-type kinase in the absence and presence of 50 μM mutant kinase were quantified and compared. Each autophosphorylation assay was performed at least twice and results were similar across duplicates.

### Measuring autophosphorylation without equilibration

For *E. coli* PhoR and *C. crescentus* PhoR, 5 μM wild-type CFP-kinase was mixed with increasing amounts of FLAG<sub>2</sub>-mutant kinase (0, 25, 50, 100 μM) in HEPES storage buffer

plus 5 mM MgCl<sub>2</sub>. After equilibration according to times established by the FRET equilibration assay (Supplementary Table 1), each mixture was autophosphorylated as in the mechanism determination assays, and autophosphorylation reactions were run for 3 min (*E. coli* PhoR) or 2 min (*C. crescentus* PhoR). Samples were separated on a 10% Tris-HCl SDS-PAGE gel and exposed to a phosphor screen as in the mechanism determination assays. In parallel, the same set of experiments was performed, but the equilibration step was omitted. Instead, FLAG<sub>2</sub>-mutant kinase was added to the wild-type CFP-kinase, and autophosphorylation was then initiated within 20 s.

### Phosphotransfer assay

Kinase chimeras were tested for their ability to phosphotransfer to *E. coli* response regulator OmpR as previously described.<sup>24</sup> CFP-histidine kinase and thioredoxin-tagged OmpR, both at 5 μM, were prepared in storage buffer plus 5 mM MgCl<sub>2</sub>. Kinases were autophosphorylated as in the mechanism determination assays, and autophosphorylation reactions were incubated for 20 min at 30 °C. Phosphotransfer was initiated by adding 2.5 μM response regulator to 2.5 μM phosphorylated kinase and reactions were stopped after 10 s, 1 min, or 5 min with sample buffer. Negative controls where no response regulator was added to the kinase were performed in identical conditions. Samples were heated for 16 min at 65 °C before being separated on a 10% Tris-HCl SDS-PAGE gel and exposed to a phosphor screen as in the mechanism determination assays.

### FRET assay to measure equilibrium dissociation constants

A previously described FRET assay was used to measure the equilibrium dissociation constants of chimera kinase homodimers, and of the heterodimers between chimera kinases and *E. coli* EnvZ.<sup>21</sup> Increasing amounts of FLAG<sub>2</sub>-mutant histidine kinase were added to an equimolar mixture of CFP-histidine kinase and YFP-histidine kinase at 0.5 μM in HEPES storage buffer. Mixtures were equilibrated in sealed 96-well plates for 8 h at 30 °C. As previously described, fluorescence was then measured and the resulting corrected FRET emission signal was used to fit homodimer or heterodimer K<sub>d</sub> values.<sup>21</sup> Each K<sub>d</sub> value was measured in duplicate. For measuring homodimer K<sub>d</sub> values, we assumed that CFP-, YFP- and mutant versions of the same histidine kinases had the same K<sub>d</sub> for dimerization. When measuring K<sub>d</sub> values for heterodimeric interactions with EnvZ, CFP-EnvZ and YFP-EnvZ were mixed with a mutant version of the interaction partner being tested. K<sub>d</sub> values were determined using a system of ordinary differential equations that described the possible equilibrium reactions between the CFP-histidine kinase, the YFP-histidine kinase, and the mutant histidine kinase.<sup>21</sup> Binding curves for different K<sub>d</sub> values were simulated with MATLAB, using a grid search over reasonable values. Each K<sub>d</sub> was then chosen so as to maximize the square of the Pearson correlation coefficient ( $R^2$ ) between the experimental data and the MATLAB-simulated data. We also estimated the range of K<sub>d</sub> values that could fit the data with similar accuracy to this best fit. The lower and upper limits of K<sub>d</sub> values that gave  $R^2$  values at least 95% as good as that of the best fit,  $R_2^{\max}$ , were calculated and are reported in Supplementary Table 2.

### Supplementary Material

Refer to Web version on PubMed Central for supplementary material.

### Acknowledgments

We thank E. J. Capra for performing the phosphotransfer control experiments. We thank T. A. Washington for providing *B. subtilis* A-168 genome DNA, E. A. Lubin and E. J. Capra for providing purified response regulators, and A. Marina for providing the *S. aureus* PhoR construct. We thank members of the Keating laboratory (especially T. S. Chen, J. B. Kaplan, C. Negron, and A. W. Reinke) and the Laub laboratory (especially E. J. Capra, A. I.

Podgornaia, and C. G. Tsokos) for insightful discussions. We thank the BioMicro Center of the Massachusetts Institute of Technology for use of the Varioskan plate reader. This work was funded by National Institutes of Health award GM067681 to A.E. Keating, a National Science Foundation CAREER Grant to M.T. Laub, and the National Science Foundation GRFP fellowship to O. Ashenberg. M.T.L. is an Early Career Scientist of the Howard Hughes Medical Institute. We used computer resources provided by National Science Foundation award 0821391.

## References

1. Stock AM, Robinson VL, Goudreau PN. Two-component signal transduction. *Annu Rev Biochem.* 2000; 69:183–215. [PubMed: 10966457]
2. Kenney LJ. How important is the phosphatase activity of sensor kinases? *Curr Opin Microbiol.* 2010; 13:168–76. [PubMed: 20223700]
3. Mascher T, Helmann JD, Uden G. Stimulus perception in bacterial signal-transducing histidine kinases. *Microbiol Mol Biol Rev.* 2006; 70:910–38. [PubMed: 17158704]
4. Gooderham WJ, Hancock RE. Regulation of virulence and antibiotic resistance by two-component regulatory systems in *Pseudomonas aeruginosa*. *FEMS Microbiol Rev.* 2009; 33:279–94. [PubMed: 19243444]
5. Moglich A, Ayers RA, Moffat K. Structure and signaling mechanism of Per-ARNT-Sim domains. *Structure.* 2009; 17:1282–94. [PubMed: 19836329]
6. Tomomori C, Tanaka T, Dutta R, Park H, Saha SK, Zhu Y, Ishima R, Liu D, Tong KI, Kurokawa H, Qian H, Inouye M, Ikura M. Solution structure of the homodimeric core domain of *Escherichia coli* histidine kinase EnvZ. *Nat Struct Biol.* 1999; 6:729–34. [PubMed: 10426948]
7. Tanaka T, Saha SK, Tomomori C, Ishima R, Liu D, Tong KI, Park H, Dutta R, Qin L, Swindells MB, Yamazaki T, Ono AM, Kainosho M, Inouye M, Ikura M. NMR structure of the histidine kinase domain of the *E. coli* osmosensor EnvZ. *Nature.* 1998; 396:88–92. [PubMed: 9817206]
8. Yang Y, Inouye M. Intermolecular complementation between two defective mutant signal-transducing receptors of *Escherichia coli*. *Proc Natl Acad Sci U S A.* 1991; 88:11057–61. [PubMed: 1662380]
9. Ninfa EG, Atkinson MR, Kamberov ES, Ninfa AJ. Mechanism of autophosphorylation of *Escherichia coli* nitrogen regulator II (NRII or NtrB): trans-phosphorylation between subunits. *J Bacteriol.* 1993; 175:7024–32. [PubMed: 8226644]
10. Filippou PS, Kasemian LD, Panagiotidis CA, Kyriakidis DA. Functional characterization of the histidine kinase of the *E. coli* two-component signal transduction system AtoS-AtoC. *Biochim Biophys Acta.* 2008; 1780:1023–31. [PubMed: 18534200]
11. Swanson RV, Bourret RB, Simon MI. Intermolecular complementation of the kinase activity of CheA. *Mol Microbiol.* 1993; 8:435–41. [PubMed: 8326858]
12. George Cisar EA, Geisinger E, Muir TW, Novick RP. Symmetric signalling within asymmetric dimers of the *Staphylococcus aureus* receptor histidine kinase AgrC. *Mol Microbiol.* 2009; 74:44–57. [PubMed: 19708918]
13. Brencic A, Xia Q, Winans SC. VirA of *Agrobacterium tumefaciens* is an intradimer transphosphorylase and can actively block vir gene expression in the absence of phenolic signals. *Mol Microbiol.* 2004; 52:1349–62. [PubMed: 15165238]
14. Pena-Sandoval GR, Georgellis D. The ArcB sensor kinase of *Escherichia coli* autophosphorylates by an intramolecular reaction. *J Bacteriol.* 2010; 192:1735–9. [PubMed: 20097862]
15. Casino P, Rubio V, Marina A. Structural insight into partner specificity and phosphoryl transfer in two-component signal transduction. *Cell.* 2009; 139:325–36. [PubMed: 19800110]
16. Presnell SR, Cohen FE. Topological distribution of four- $\alpha$ -helix bundles. *Proc Natl Acad Sci U S A.* 1989; 86:6592–6. [PubMed: 2771946]
17. Marina A, Waldburger CD, Hendrickson WA. Structure of the entire cytoplasmic portion of a sensor histidine-kinase protein. *Embo J.* 2005; 24:4247–59. [PubMed: 16319927]
18. Ferris HU, Dunin-Horkawicz S, Hornig N, Hulko M, Martin J, Schultz JE, Zeth K, Lupas AN, Coles M. Mechanism of regulation of receptor histidine kinases. *Structure.* 2012; 20:56–66. [PubMed: 22244755]
19. Casino P, Rubio V, Marina A. The mechanism of signal transduction by two-component systems. *Curr Opin Struct Biol.* 2010; 20:763–71. [PubMed: 20951027]

20. Zhu Y, Inouye M. The role of the G2 box, a conserved motif in the histidine kinase superfamily, in modulating the function of EnvZ. *Mol Microbiol.* 2002; 45:653–63. [PubMed: 12139613]
21. Ashenberg O, Rozen-Gagnon K, Laub MT, Keating AE. Determinants of homodimerization specificity in histidine kinases. *J Mol Biol.* 2011; 413:222–35. [PubMed: 21854787]
22. Cai SJ, Inouye M. Spontaneous subunit exchange and biochemical evidence for trans-autophosphorylation in a dimer of *Escherichia coli* histidine kinase (EnvZ). *J Mol Biol.* 2003; 329:495–503. [PubMed: 12767831]
23. Park SY, Quezada CM, Bilwes AM, Crane BR. Subunit exchange by CheA histidine kinases from the mesophile *Escherichia coli* and the thermophile *Thermotoga maritima*. *Biochemistry.* 2004; 43:2228–40. [PubMed: 14979719]
24. Skerker JM, Prasol MS, Perchuk BS, Biondi EG, Laub MT. Two-component signal transduction pathways regulating growth and cell cycle progression in a bacterium: a system-level analysis. *PLoS Biol.* 2005; 3:e334. [PubMed: 16176121]
25. Trajtenberg F, Grana M, Ruetalo N, Botti H, Buschiazzo A. Structural and enzymatic insights into the ATP binding and autophosphorylation mechanism of a sensor histidine kinase. *J Biol Chem.* 2010; 285:24892–903. [PubMed: 20507988]
26. Bryson K, McGuffin LJ, Marsden RL, Ward JJ, Sodhi JS, Jones DT. Protein structure prediction servers at University College London. *Nucleic Acids Res.* 2005; 33:W36–8. [PubMed: 15980489]
27. Pal L, Dasgupta B, Chakrabarti P. 3(10)-Helix adjoining alpha-helix and beta-strand: sequence and structural features and their conservation. *Biopolymers.* 2005; 78:147–62. [PubMed: 15759287]
28. Bick MJ, Lamour V, Rajashankar KR, Gordiyenko Y, Robinson CV, Darst SA. How to switch off a histidine kinase: crystal structure of *Geobacillus stearothermophilus* KinB with the inhibitor Sda. *J Mol Biol.* 2009; 386:163–77. [PubMed: 19101565]
29. Yamada S, Sugimoto H, Kobayashi M, Ohno A, Nakamura H, Shiro Y. Structure of PAS-linked histidine kinase and the response regulator complex. *Structure.* 2009; 17:1333–44. [PubMed: 19836334]
30. Wang LC, Morgan LK, Godakumbura P, Kenney LJ, Anand GS. The inner membrane histidine kinase EnvZ senses osmolality via helix-coil transitions in the cytoplasm. *Embo J.* 2012; 31:2648–59. [PubMed: 22543870]
31. Capra EJ, Laub MT. Evolution of Two-Component Signal Transduction Systems. *Annu Rev Microbiol.* 2012
32. Skerker JM, Perchuk BS, Siryaporn A, Lubin EA, Ashenberg O, Goulian M, Laub MT. Rewiring the specificity of two-component signal transduction systems. *Cell.* 2008; 133:1043–54. [PubMed: 18555780]
33. Capra EJ, Perchuk BS, Skerker JM, Laub MT. Adaptive Mutations that Prevent Crosstalk Enable the Expansion of Paralogous Signaling Protein Families. *Cell.* 2012; 150:222–32. [PubMed: 22770222]
34. Larkin MA, Blackshields G, Brown NP, Chenna R, McGettigan PA, McWilliam H, Valentin F, Wallace IM, Wilm A, Lopez R, Thompson JD, Gibson TJ, Higgins DG. Clustal W and Clustal X version 2.0. *Bioinformatics.* 2007; 23:2947–8. [PubMed: 17846036]
35. Crooks GE, Hon G, Chandonia JM, Brenner SE. WebLogo: a sequence logo generator. *Genome Res.* 2004; 14:1188–90. [PubMed: 15173120]
36. Punta M, Coggill PC, Eberhardt RY, Mistry J, Tate J, Boursnell C, Pang N, Forslund K, Ceric G, Clements J, Heger A, AHolm L, Sonnhammer EL, Eddy SR, Bateman A, Finn RD. The Pfam protein families database. *Nucleic Acids Res.* 2012; 40:D290–301. [PubMed: 22127870]
37. Grebe TW, Stock JB. The histidine protein kinase superfamily. *Adv Microb Physiol.* 1999; 41:139–227. [PubMed: 10500846]
38. Gao R, Tao Y, Stock AM. System-level mapping of *Escherichia coli* response regulator dimerization with FRET hybrids. *Mol Microbiol.* 2008; 69:1358–72. [PubMed: 18631241]



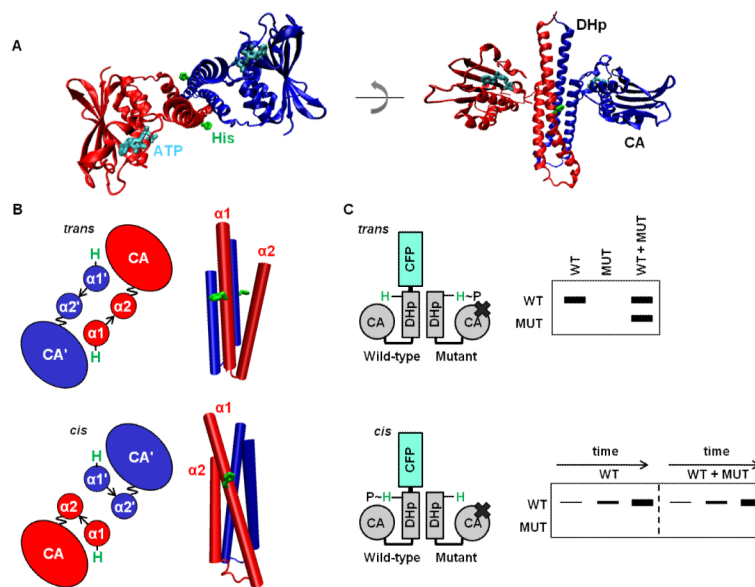


### Figure 1. Histidine kinases autophosphorylate in *cis* or in *trans*

(A) The cytoplasmic region of a histidine kinase (PDB ID 2C2A) consists of conserved DHp and CA domains. The histidine site of phosphorylation on the DHp domain, and the ATP analog bound by the CA domain, are shown in stick form in green and cyan, respectively. The kinase shown autophosphorylates in *cis*. (B) Cartoon (left) looking down the four-helix bundle (right) of the DHp-domain dimer. The  $\alpha 1$  and  $\alpha 2$  helices in the DHp domain are labeled, with the prime symbol (') symbol denoting the opposite chain (top: PDB ID 3ZRX, bottom: PDB ID 2C2A). The loop at the base of the DHp domain is depicted by an arrow, and the linker between the DHp and CA domains is depicted as a wavy line to reflect the mobility of the CA domain. Depending on loop handedness in the DHp domain, the CA domain is either closer to the histidine on the same chain (*cis*) or the histidine on the opposite chain (*trans*). (C) Schematic of the assay to test in *cis* vs. in *trans* autophosphorylation. A wild-type (WT) histidine kinase homodimer is mixed with excess mutant (MUT) histidine-kinase homodimer unable to bind ATP. Autophosphorylation within the heterodimer is initiated by the addition of radiolabeled ATP, and the chains in the dimer are then separated by SDS-PAGE. In the heterodimer, either the WT or MUT chain is labeled, depending on whether the kinase autophosphorylates in *cis* or in *trans*, respectively. In addition, WT homodimer, also present in the WT+MUT mixture, undergoes autophosphorylation. To confirm autophosphorylation in *cis*, the kinetics of the WT and WT plus excess MUT reactions are compared.



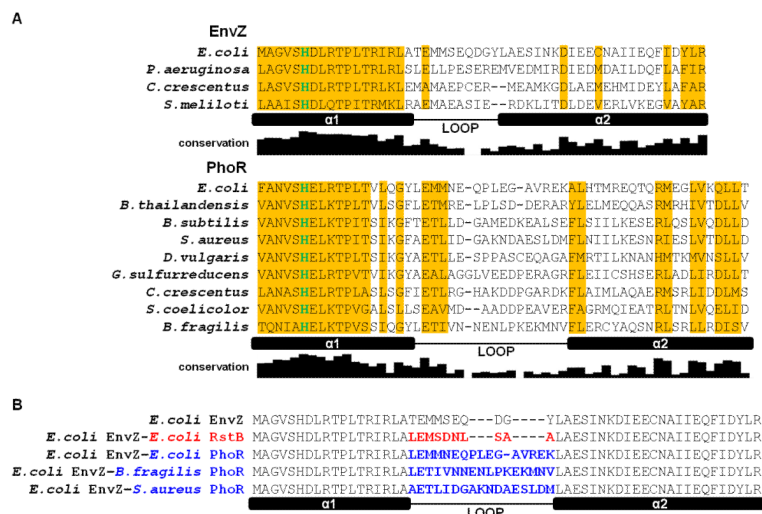


**Figure 2. Alignments of EnvZ and PhoR orthologs and loop chimeras**

(A) Sequence alignment of DHP domains from EnvZ and PhoR orthologs characterized in this study. Locations of the two helices in the DHP domain,  $\alpha 1$  and  $\alpha 2$ , and the loop connecting them are indicated. The depicted ortholog loop boundaries are based on sequence alignment to *E. coli* EnvZ and its loop boundary. The histidine site of phosphorylation is colored in green. Columns where one residue is conserved in more than half of 118 EnvZ or 385 PhoR orthologs are shaded in yellow. The conservation graph below each alignment measures information for each DHP position across all orthologs (see Methods). (B) Alignment of DHP domains of loop chimeras. Sequence changes relative to *E. coli* EnvZ are highlighted in either red (RstB) or blue (PhoR).

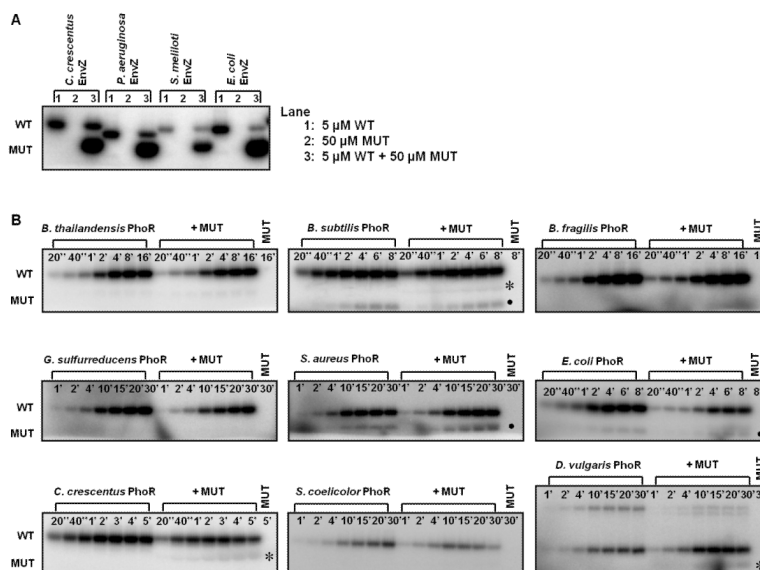


**Figure 3. Autophosphorylation mechanism within EnvZ and PhoR orthologs is conserved**  
 (A) Characterization of autophosphorylation mechanism for EnvZ orthologs. In each ortholog series, the first gel lane contained 5  $\mu$ M wild-type (WT) kinase, the second lane contained 50  $\mu$ M mutant (MUT) kinase, and the third lane contained a mixture of the two kinases. The mixture was incubated for four hours at 30  $^{\circ}$ C before initiating autophosphorylation. (B) Characterization of autophosphorylation mechanism for PhoR orthologs. The gel for each ortholog included two autophosphorylation time courses: the first for 5  $\mu$ M wild-type kinase alone and the second for 5  $\mu$ M wild-type kinase plus 50  $\mu$ M mutant kinase. The final lane contained 50  $\mu$ M mutant kinase. The autophosphorylation time is marked in each lane. Asterisks indicate possible weak in *trans* autophosphorylation, and solid circles mark a breakdown product found in both the WT and WT + MUT reactions. The slower mobility band seen with *D. vulgaris* PhoR is a PhoR dimer. Gel images were quantified and are plotted in Supplementary Fig. 2.

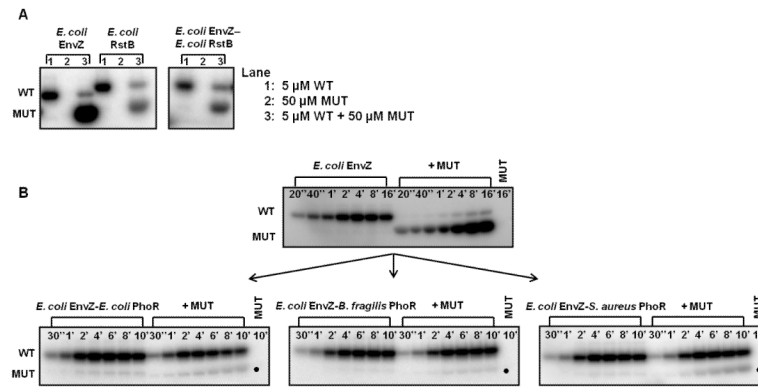


**Figure 4. Changing DHP loop sequence changes autophosphorylation mechanism**  
 (A) Characterization of autophosphorylation mechanism in *E. coli* EnvZ, *E. coli* RstB, and the EnvZ-RstB chimera, as in Fig. 3A. (B) Autophosphorylation time courses for *E. coli* EnvZ and the EnvZ-PhoR loop chimeras, as in Fig. 3B. Gel images were quantified and are plotted in Supplementary Fig. 4.

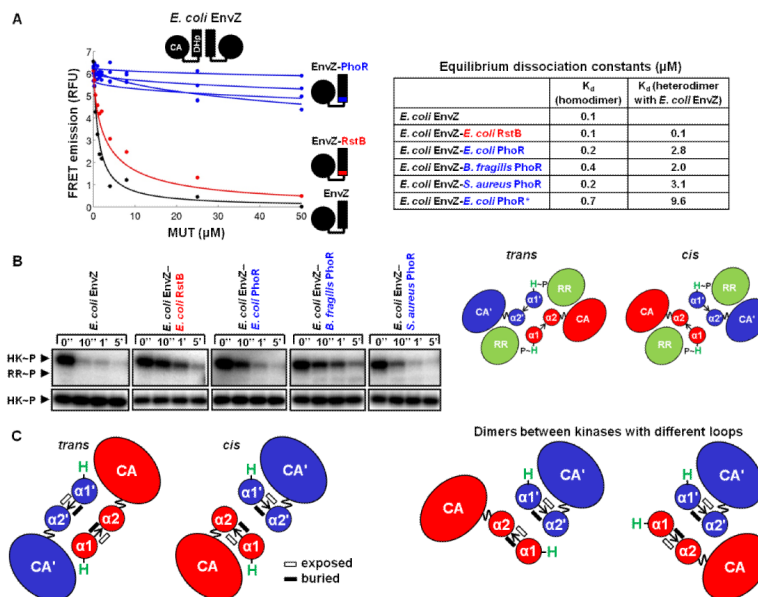


**Figure 5. Phosphotransfer specificity and dimerization specificity of loop chimeras**  
 (A) Each kinase was assayed for its ability to interact with *E. coli* EnvZ using a FRET competition assay. FRET signal from a complex of CFP-EnvZ and YFP-EnvZ was disrupted by interaction with unlabeled mutant (MUT) kinase (*E. coli* EnvZ, EnvZ-RstB chimera, EnvZ-PhoR loop chimeras, or *E. coli* EnvZ-*E. coli* PhoR\*). Equilibrium dissociation constants ( $K_d$ ) were fit for each kinase homodimer and for each kinase heterodimer with EnvZ. (B) *E. coli* EnvZ and the EnvZ loop chimeras were assayed for their ability to phosphotransfer to the response regulator (RR) *E. coli* OmpR. Autophosphorylated histidine kinase (HK) was incubated for the indicated times with OmpR either present (top gel) or absent (bottom gel). Each kinase was able to phosphotransfer to OmpR, as seen by decreased levels of autophosphorylated kinase upon incubation with OmpR. On the right are cartoon depictions of a response regulator interacting with the DHp domain dimer of a kinase that phosphorylates in *trans* (left) or in *cis* (right). The mode of interaction in the *cis* kinase is based on a crystal structure (PDB ID 3DGE), and the mode of interaction in the *trans* kinase is a model. (C) A DHp dimer formed between chains with different loop handedness cannot form the stereotypical DHp interface. In such a dimer, either the usual buried dimer interface (represented by solid black rectangles) will not be formed, or the arrangement of the  $\alpha 1$  and  $\alpha 2$  helices will be altered from what is observed in known structures.